Frequency Response Analysis of the Unsteady-State CO/CO_2 Methanation Reaction: An Experimental Study

*Dominik Meyer, Jannik Schumacher, Jens Friedland, Robert Güttel**

Ulm University, Albert-Einstein-Allee 11, 89081 Ulm, Germany

E-mail address: robert.guettel@uni-ulm.de

Abstract

The utilization of renewable electricity for power-to-gas (PtG) applications induces fluctuations in the H_2 availability from water electrolysis. For subsequent methanation of CO or CO_2 the unsteady-state operation of the respective reactor allows to minimize H_2 storage capacities. However, the impact of temporal fluctuations in feed gas composition on the methanation reaction and the respective transient kinetics has not yet been fully understood. We investigated the methanation of various CO/CO_2 (CO_x) feed gas mixtures under periodically changing gas compositions with emphasis on the effect of the frequency on the reactor response. We show that the frequency response of CH_4 exhibits a characteristic hysteresis, which depends on the switching direction between CO_x-lean and CO_x-rich feeds and their composition. From the shape of the hysteresis we are able to conclude on the preferred CO_x species being hydrogenated to CH_4 under respective conditions, which also provides mechanistic insights. By applying high cycling

frequencies, the highly reactive species present under CO methanation conditions can even selectively be activated, which explains the higher reactivity compared to steady-state conditions reported, frequently.

List of Symbols

Symbol	Description	Unit
Latin letters		
d_p	Particle size	µm
E	Rate enhancement factor	1
F	Step response	1
m_cat	Catalyst mass	mg
M	Magnitude	dB
N	Number	1
$\dot{n}$	Molar flow rate	mol s^{-1}
$\bar{\dot{n}}$	Average molar flow rate	mol s^{-1}
$\hat{\dot{n}}$	Amplitude of the molar flow rate	mol s^{-1}
p	Operating or partial pressure	bar
R	Universal gas constant	J mol^{-1} K^{-1}
s	Cycle split	1
t	Time	s
T	Operating temperature	K
t	Time	s
$\dot{V}$	Volumetric flow rate at standard temperature and pressure	mL_{STP} min^{-1}
x	Molar fraction	1
z	CO/CO_2 feed ratio	1
Greek letters		
α	Volume variation factor	1
θ	Normalized time within one limit cycle	1
τ	Cycle period duration	s
τ_C	Characteristic relaxation time	s
Subscripts		
0	Initial	
1, 2	Initial / final steady-state	
dil	Dilution	
i	Component i	

in	Inlet
j	Number of limit cycle
LC	Limit cycle
out	Outlet
RTD	Residence time distribution
ref	Reference
STP	Standard temperature and pressure
ss	Steady-state
trans	Transient

1 INTRODUCTION

With the Power-to-X technology the possibility arises to convert surplus fluctuating renewable electricity into chemical energy. Especially the storage of electrical energy in synthetic natural gas (SNG) via the Power-to-Gas process (PtG) is a promising option for temporal decoupling of energy availability and demand.[1–3] Therefore, H_2 is produced from electrical energy via water electrolysis, which is subsequently used for methanation of carbon oxides available from various sources. For instance, by utilizing industrial exhaust gases as carbon sources the potential to convert highly concentrated CO_2 into CH_4 directly at the emitting spot reduces the effort for CO_2 separation prior to hydrogenation. However, these exhaust gases may also contain CO, i.e. blast furnace or converter gas in steel making.[4] Both carbon oxides can be hydrogenated into CH_4 using solid catalysts (e.g. Ni/Al_2O_3) via the stoichiometric reactions (1) and (2).[5]

$$CO_2 + 4H_2 \rightleftharpoons CH_4 + 2\,H_2O \quad (1)$$

$$CO + 3H_2 \rightleftharpoons CH_4 + H_2O \quad (2)$$

From an economic viewpoint the implementation of decentralized small-scale methanation plants in proximity of carbon point sources associated with available renewable energy sources is advantageous.[2] Such units, however, require minimal upstream buffer capacities to be cost-effective. This consequently leads to a propagation of fluctuations in reactant availability and composition into the reactor, which is the case for both H_2 and the CO/CO_2 source. Hence, the

methanation reactor needs to be operated under unsteady-state conditions for such cases with respect to fluctuations in the feed gas composition and volumetric flowrate, which induce a complex non-linear interaction of kinetic processes in the methanation reactor occurring at different length scales.[1,6] Moreover, the input fluctuations can appear stochastically over a wide frequency range,[1] which may result in a complex reactor behavior depending on the input frequencies.[7] Dynamic changes in the inlet composition, however, may also affect the thermal behavior of the methanation reactor, since the hydrogenation of CO and CO_2 is highly exothermic. In order to avoid unstable operation regimes induced by moving hot spots[8–10] or wrong way behavior,[11] different temperature control strategies were developed for unsteady-state methanation reactors.[12–16] For instance, Theurich et al. used the product recycle in a loop reactor setup as an additional control parameter, which is capable to dampen the temperature increase after step changes of the flow rate.[13–15] Bremer and Sundmacher showed theoretically that by adaptive controlling the coolant temperature a CO_2 methanation reactor can be operated in an unstable operation point yielding high CO_2 conversions at moderate catalyst temperatures.[12] On the catalyst scale, the focus is on the stability of the active compound,[17,18] as well as the optimal shape of the pellets to buffer fluctuations.[19]

In order to unfold the unsteady-state reactor behavior, the evaluation of the frequency-dependent reactor response, also referred to as frequency response, is in the focus of the present contribution assuming isothermal conditions. The frequency response can, in principle, be classified based on the ratio between the cycle period duration τ and the characteristic relaxation time τ_C into the following three regimes:[6,20,21]

- quasi-steady-state (qss) regime ($\tau \gg \tau_C$): The reactor response is able to reach steady-state in each half-period of the forced periodic input, since the kinetic processes are fast enough

compared to the cycle period. Thus, the amplitude of the forced input signal is not damped by the system.

- relaxed steady-state (rss) regime ($\tau \ll \tau_C$): The large characteristic time of relaxation compared to that of the forced input leads to damping and thus to an averaging of the system response over the duration of a period.
- full-transient state (fts) regime ($\tau \cong \tau_C$): The transition between the qss and the rss regime is characterized by a strong sensitivity of the system response on the cycle period of the forced input signal.

Based on the applied input frequency performance enhancement[21–25] or even resonance effects[26] can occur. The nonlinear frequency response (NFR) analysis, for example, allows an *a piori* screening of possible rate enhancement with periodic reactor operation based on the prediction of the average composition and flow rates of the reactor outlet stream.[27,28] Therefore, a validated kinetic and reactor model applicable to dynamic operation conditions is required. The theoretical analysis of the resulting non-linear reactor model allows to determine the possible rate enhancement depending on the applied frequency and the phase shift between two input parameters (if two parameters are modulated). However, for experimental validation of the theoretical predictions a sophisticated experimental setup and respective procedures are required, as we pointed out, recently.[6] The aforementioned NFR method was applied to the methanation reaction and predicts rate enhancement for CO and CO_2 methanation.[29,30] For CO methanation various authors have confirmed experimentally that a higher CH_4 yield is possible under periodic operation compared to optimized steady-state conditions.[31–33] For CO_2-methanation, in contrast, a yield enhancement was not yet confirmed experimentally.[34,35]

In all these experimental and theoretical studies, however, the underlying phenomena responsible for the observed performance enhancement have not yet been fully understood. In particular, the effect of the forcing frequency on the kinetic processes taking place on the catalyst surface, e.g. ad-/desorption and surface reaction remains unclear. Consequently, the objective of this study is the experimental investigation of the frequency response of the CO/CO_2 methanation in order to correlate mechanistic effects on the catalyst surface to possible performance enhancement. Therefore, we vary the frequency of the inlet gas composition by switching between a CO_x-rich and a CO_x-lean feed gas and evaluate the corresponding reactor response using the Periodic Transient Kinetics (PTK) method introduced in our recent work.[6] In particular, the whole range of CO/CO_2 ratios are covered experimentally in order to deduce the effect of competing ad-/desorption and reaction steps involved in simultaneous CO/CO_2 methanation on the dynamic response. The observed effect of the forcing frequency is discussed with respect to mechanistic aspects characteristic for both CO and CO_2 hydrogenation, whose behavior is considered to be distinct from each other as presumed from our previous steady-state experiments[5].

2 MATERIAL AND METHODS

2.1. Catalyst

The 5 wt-% Ni/A_2O_3 catalyst is synthesized via the incipient wetness impregnation method of 800 µm Al_2O_3 particles (Puralox® Al_2O_3-Spheres 0.8/160, Sasol Germany) by aqueous $Ni(NO_3)_2$ solution. After crushing and sieving a particle size fraction of 150 – 200 µm is selected for the experimental studies. The specific surface area of 167 $m^2 g_{cat}^{-1}$ and the average pore diameter of 8 nm is determined by N_2 physisorption measurements (3Flex, micromeritics). Based on chemisorption measurements (3Flex, micromeritics) the H_2 adsorption capacity is calculated to be 48 $\mu mol\ g_{cat}^{-1}$. Assuming dissociative H_2 adsorption as well as spherical Ni nanoparticles, a metal

surface area of 3.7 $m^2\ g_{cat}^{-1}$, a crystallite size of 7.5 nm and a metal dispersion of 14.2 % is determined. Moreover, the measurements show that due to crushing the morphologic properties do not change. More information about the catalyst synthesis and characterization can be found elsewhere.[5]

2.2. Experimental setup

Since the experimental setup is described in detail previously,[6] only a brief overview is given here. The experiments are conducted in a stainless-steel fixed-bed reactor with an inner diameter of 4.5 mm and a total length of 30 cm. The catalyst sample of 50 mg is diluted with 100 mg of inert material of the same size (Al_2O_3, Sasol Puralox). The resulting packed-bed (ca. 2 cm length) is placed in the center of the isothermal zone (ca. 10 cm length). For temperature measurement the reactor tube is equipped with a concentric 1/16-inch capillary containing a moveable thermocouple. Isothermal conditions are ensured by dilution of the gas flow with He and of the active catalyst particles by inert Al_2O_3. Measurements in the catalyst bed under reactive conditions confirm a constant temperature within a ±1.5 K range for all experiments. The catalyst packing is framed by 1.2 g glass particles (150 – 200 µm) on top (ca. 5 cm length) and 0.6 g below (ca. 2.5 cm length) to ensure homogenous flow pattern within the catalyst section. The whole packing is fixed in place by quartz wool. The gases are continuously supplied by two separate lines, which can automatically be switched by means of a pneumatic 4/2 way-valve (Fitok). The gases are provided from top with separate mass flow controllers (EL-FLOW Prestige, Bronkhorst) for each component and supply line. Hence, the feed gas compositions can individually be configured with H_2 (5.0 purity, MTI), CO/Ar (10 vol.-% Ar 5.0 purity in CO 3.8 purity, Air Liquide), CO_2 (4.8 purity, MTI), Ar (5.0 purity, MTI) and He (5.0 purity, MTI) in all possible compositions.

Directly downflow the reactor the effluent is diluted with a mixture of H_2 (5.0, MTI) and Ne (5.0, MTI) and subsequently subjected to the analytics consisting of a gas chromatograph (GC, GC-2010, Shimadzu) and a mass spectrometer (MS, Cirrus 3-XD, MKS). The section between reactor and analytics is kept short and is heated to prevent condensation of H_2O. The MS analyzes the calibrated (regular calibration by auxiliary GC measurements) mass-to charge ratios 2 (H_2), 15 (CH_4), 18 (H_2O), 28 (CO and CO_2), 40 (Ar), and 44 (CO_2) quantitatively, while higher hydrocarbons (26: C_2H_6 and C_3H_8, 43: C_3H_8) are monitored qualitatively, as well. The calibration for H_2O is performed *in situ* under pure CO methanation conditions at 556 K and in steady-state. It is assumed that H_2O and CH_4 are produced in stoichiometric amounts, due to the absence of the water-gas-shift reaction and a CH_4 selectivity exceeding 94 %.[5,36,37] Furthermore, adsorption of H_2O at the tubing walls is neglected.

2.3. Experimental procedure

The influence of the cycle period duration on the methanation reaction is studied under the reaction conditions given in Table 1, where a differential reactor operation is ensured by keeping the total carbon oxide conversion below 20 %.[38] The absence of intra- and inter-particle heat and mass transport limitations is confirmed applying the Mears, Anderson and Carberry criterion according to our previous study.[5] Furthermore, equilibrium effects can be excluded in this temperature range,[37] rendering the reaction being irreversible under the conditions studied.

The forced concentration cycling is performed applying 50 step changes in the feed gas composition periodically by switching between the feed gas line 1 and 2 and vice versa. The half-period for each line to be contacted with the catalyst is equal, which corresponds to a cycle split $s = 0.5$ for all experiments. The experimental procedure distinguishes between experimental runs

and single experiments. Experimental runs are conducted at different temperatures and CO_x ratios, each consisting of several single experiments at different cycle period durations τ.

The compositions used in both gas feed lines are summarized in Table 2. Note that line 1 consists of a CO_x/H_2 mixture, while line 2 is CO_x free. The applied CO/CO_2 feed ratio is described with the parameter z, according to eq. (3) with the constant reference partial pressure of $p_{\mathrm{ref}} = 0.2$ bar. The z values of 0, 0.1, 0.5, and 1 are studied experimentally, since these values are characteristic for different regimes of the methanation reaction kinetics as reported in our previous work.[5]

$$z = \frac{p_{\mathrm{CO,in}}}{p_{\mathrm{ref}}} = 1 - \frac{p_{\mathrm{CO_2,in}}}{p_{\mathrm{ref}}} \tag{3}$$

In order to ensure a comparable catalyst state, the catalyst is treated with a H_2/He flow equivalent to the composition of feed line 2 for 15 min between each single experiment. Between the experimental runs the catalyst is regenerated for 4 h under flowing H_2 ($125\ \mathrm{mL_{STP}\ min^{-1}}$), where the catalyst remained at least for 1 h at 603 K.

Table 1: Operating conditions.

Parameter	Symbol	Unit	Value
Catalyst mass	m_{cat}	mg	50
Particle size	d_{p}	µm	200
Total inlet flow rate	$\dot{V}_{\mathrm{in,STP}}$	$\mathrm{mL_{STP}\ min^{-1}}$	250
Dilution flow rate (H_2/Ne)	$\dot{V}_{\mathrm{dil,STP}}$	$\mathrm{mL_{STP}\ min^{-1}}$	245/5
Operation temperature	T	K	533-576
Operating pressure	p	bar	2
Cycle period duration	τ	s	6-240
Cycle split	s	1	0.5

Table 2: Composition of gas feed line 1 and 2 (inlet partial pressure $p_{i,\mathrm{in}}$ of component i).

Component	Unit	Inlet partial pressure $p_{i,\mathrm{in}}$
		Feed gas line 1
He	bar	0.98
H_2	bar	0.80
CO_x	bar	0.20
Ar	bar	0.02
		Feed gas line 2
He	bar	1.20
H_2	bar	0.80

2.4. Data evaluation

The data evaluation is performed as described in detail in our recent publication introducing the periodic transient kinetics method.[6] In particular, the external standard Ne is used for determining the outlet molar flow rate. Therefore, the volume variation factor α is calculated from the measured (x_{Ne}) and the initial ($x_{\mathrm{Ne},0}$) molar fraction of Ne at the reactor outlet according to eq. (4), which describes the volume variation during the methanation reaction. The outlet molar flow rate of each component i under reaction conditions, $\dot{n}_{i,\mathrm{out}}$, can now be obtained via eq. (5) based on measured outlet molar fractions $x_{i,\mathrm{out}}$. R is the universal gas constant, while p_{STP}, T_{STP} and $\dot{V}_{\mathrm{STP,in}}$ are the pressure, the temperature and the inlet volumetric flow rate under standard conditions.

$$\alpha(t) = \frac{x_{\mathrm{Ne},0}}{x_{\mathrm{Ne}}(t)} \tag{4}$$

$$\dot{n}_{i,\mathrm{out}}(t) = \alpha(t)\, x_{i,\mathrm{out}}(t) \frac{p_{\mathrm{STP}}\, \dot{V}_{\mathrm{STP,in}}}{R\, T_{\mathrm{STP}}} \tag{5}$$

For statistical analysis of the periodic response the last N_{LC} consecutive limit cycles of each single experiment are used, in order to calculate the average outlet molar flow rate of each component $\bar{\dot{n}}_{i,\mathrm{out}}(t)$ according to eq. (6). Typically, the outlet molar flow rate $\dot{n}_{i,j,\mathrm{out}}$ for component i in limit cycle j is averaged over last 25 limit cycles. The obtained result thus corresponds to the average limit cycle, which is subject to scientific discussion and denoted as $\dot{n}_i$ in the following for simplification.

$$\dot{n}_i(t) = \bar{\dot{n}}_{i,\mathrm{out}}(t) = \frac{1}{N_{\mathrm{LC}}} \sum_{j=1}^{N_{\mathrm{LC}}} \dot{n}_{i,j,\mathrm{out}}(t) \tag{6}$$

Ar is used as internal standard in order to measure the residence time distribution (RTD) in each individual experiment. The application of eq. (7) than allows to discriminate the effect of the RTD $\dot{n}_{i,\mathrm{RTD}}$ in the measured transient reactor response $\dot{n}_i$ from the interaction of gaseous components with the solid surface expressed by transient molar flow rate $\dot{n}_{i,\mathrm{trans}}$.

$$\dot{n}_i(t) = \dot{n}_{i,\mathrm{RTD}}(t) + \dot{n}_{i,\mathrm{trans}}(t) \tag{7}$$

$$\dot{n}_{i,\mathrm{RTD}}(t) = F_{\mathrm{Ar}}(t)\,(\dot{n}_{i,\mathrm{ss},2} - \dot{n}_{i,\mathrm{ss},1}) + \dot{n}_{i,\mathrm{ss},1} \tag{8}$$

$$F_i(t) = \frac{\dot{n}_i(t) - \dot{n}_{i,\mathrm{ss},1}}{\dot{n}_{i,\mathrm{ss},2} - \dot{n}_{i,\mathrm{ss},1}} \tag{9}$$

In order to determine the response for each component expected from RTD the step-response F_{Ar} is required, according to eq. (8). Since Ar is assumed to not interact with the solid surface, due to negligible ad-/desorption, $\dot{n}_{\mathrm{Ar,trans}}$ equals zero and hence Ar represents the RTD of the system. Thus eq. (9) allows to determine the step-response of the system from the measured response of the internal standard. The steady-state values for both half-periods $\dot{n}_{i,\mathrm{ss},2}$ and $\dot{n}_{i,\mathrm{ss},1}$ required in eqs. (8) and (9) are determined from averaging the last 10 s for each half period at a period duration of 240 s.

The rate enhancement factor E is determined by eq. (11), which requires the average CH_4 outlet molar flow rate ($\dot{n}_{\mathrm{CH_4,LC}}$) during the average limit cycle (eq. (10)) and the steady-state value $\dot{n}_{\mathrm{CH_4},\mathrm{ss},2}$ corresponding to the CO_x rich half period 1.

$$\dot{n}_{\mathrm{CH_4,LC}} = \frac{1}{\tau}\int_0^{\tau} \dot{n}_{\mathrm{CH_4}}(t)\ dt \tag{10}$$

$$E = \frac{\dot{n}_{\mathrm{CH_4,LC}}}{\dot{n}_{\mathrm{CH_4,ss,2}}} \tag{11}$$

The magnitude M of the frequency response is determined from the amplitude $\hat{\dot{n}}_i$ of the response for each individual component i. First, the amplitude is calculated from the outlet molar flow rates via eq. (12). The magnitude is then obtained with eq. (13), which relates the amplitude to that of the reference case $\hat{\dot{n}}_{i,\mathrm{ref}}$ with a cycle period duration of 240 s.

$$\hat{\dot{n}}_i = \max[\dot{n}_i(t)] - \dot{n}_{i,\mathrm{LC}} \tag{12}$$

$$M_{\mathrm{i}} = 20\log\frac{\hat{\dot{n}}_i}{\hat{\dot{n}}_{i,\mathrm{ref}}} \tag{13}$$

3 EXPERIMENTAL RESULTS AND DISCUSSION

3.1. Effect of cycle period duration on the reactant response

Figure 1 shows the individual outlet molar flow rates of the reactants CO and CO_2, as well as those of the products CH_4 and H_2O in the limit cycle for different cycle period durations in a range between 6 and 240 s. The CO_x mixture is chosen to fulfill $z = 0.1$, since a simultaneous conversion of CO and CO_2 can be expected for that value based on steady-state experiments.[5] For $\tau = 240\ s$ (blue lines) all components are reaching steady-state, which means that the system is in the *qss* regime concerning all components and which also provides the reference for calculating the magnitude in eq. (13). Reducing τ leads to a decreasing measured amplitude, though the input amplitude is constant. Furthermore, this affect is differently pronounced for the components

studied. For instance, the amplitude of CO and CO_2 shrinks only slightly upon reducing the cycle period duration to 30 s indicating that both components remain in the *qss* regime. In contrast, the amplitudes of H_2O and CH_4 are clearly damped for $\tau = 30$ s, already. Further reduction of the cycle period durations leads to a shift for CO and CO_2 into the *fts* regime, while H_2O appears to even reach the *rss* regime for τ =6 s indicated by the almost constant signal during the whole limit cycle.

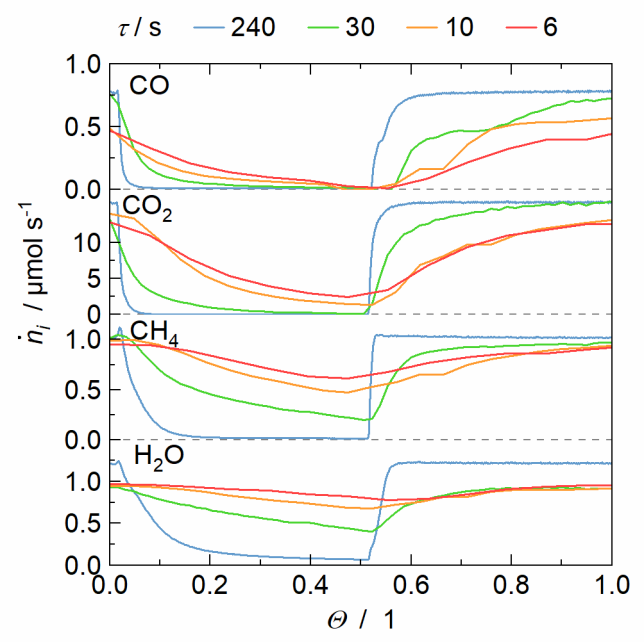

Figure 1: Outlet molar flow rate of the reactants $\dot{n}_i$ for different cycle period durations τ as function of the normalized time within the limit cycle $\theta = t/\tau$ (reaction conditions: z = 0.1, 556 K, 2 bar).

The effect of the cycle period duration on the reactant response is depicted in Figure 2 by plotting the magnitude M_i for each component. The response for the internal standard Ar represents the real RTD including the dynamic transport processes at the macro and meso scale.[6] It can be observed that the magnitude is constant for cycle period durations above 30 s and decreases with a constant slope of 6 dB/decade below durations of 30 s. This clearly indicates that the Ar response is in the *qss* regime for long cycle periods and shifts into the *fts* regime below 30 s. The observed

trends for CO and CO_2 are rather similar Ar, particularly regarding the slope of ca. 6 dB/decade for cycle period durations below 30 s. The similar slope in magnitude for CO, CO_2 and Ar suggests that the respective response is governed by the systems RTD, which is expected for reactants as predicted by Meyer et al. for simplified cases.[7]

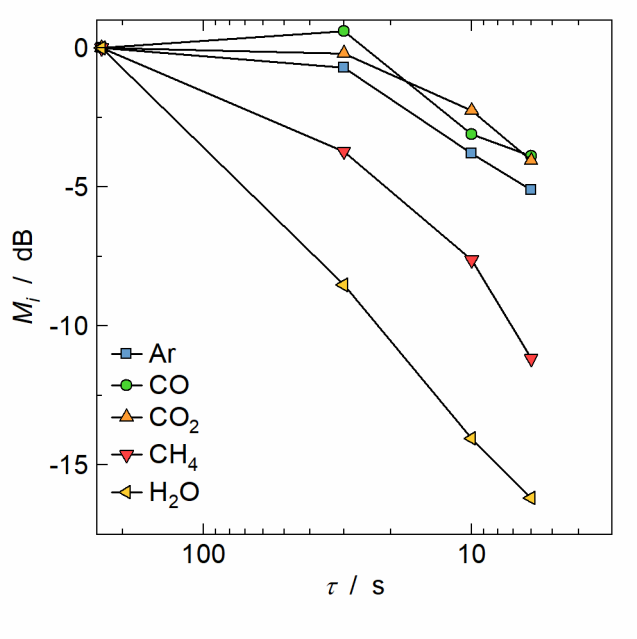

Figure 2: Magnitude M_i of the outlet molar flow rate for each component as function of the cycle period duration τ (reaction conditions: z = 0.1, 2 bar, 556 K).

In contrast, the trends for CH_4 and H_2O differ significantly. The H_2O magnitude decreases by 11 dB/decade over the whole range of cycle period durations, while the CH_4 magnitude seems to exhibit different slopes, the average of 7 dB/decade being between those of H_2O and Ar. The decreasing slopes for CH_4 and H_2O compared to Ar are expected from our theoretical considerations,[7] since both components are formed by reaction. Interestingly, the slopes of CH_4 and H_2O differ from each other, though both are formed simultaneously. This contradiction can be explained by an instantaneous desorption of CH_4 from the solid surface upon formation, while H_2O remains adsorbed for a certain time. In principle, this consideration agrees with our

experimental results obtained for a fixed cycle period duration of 240 s, where a delay of the H_2O response is reported compared to CH_4.[39] Furthermore, a high sorption capacity of the active and support material is known for H_2O[40], which is responsible for the delayed desorption.

From the effect of the cycle period duration on the magnitude of all components considered here it can be concluded that the reactor system is capable for damping of the inlet fluctuations, in particular for fast changes. The reactor volume, characterized by its RTD, acts as respective buffer for that purpose. For the products, the solid surface provides additional buffer storage leading to even more pronounced damping of the inlet fluctuations. An additional damping effect of the solid surface for CO_x species, however, was not observed in the present work. Therefore, an individual characteristic time $\tau_{i,C}$ obviously exists for each component.

3.2. Frequency response of CH_4

The impact of the cycle period duration on the CH_4 response in the limit cycle is depicted in Figure 3. The steady-state values for each experimental run are determined from the experiments with a cycle period duration of 240 s (see reference case for eq. (13)) and are displayed as black and grey diamonds. The course of the CH_4 response within a limit cycle for each specific value for τ is characterized by a hysteresis between the CO_x-lean (solid lines) and the CO_x-rich phase (dashed lines). Since the CH_4 response increases after switching to the CO_x-rich phase and exhibits a delay of the measured compared to the expected values, the trajectory in the state space plot (Figure 3b)) develops in counter-clockwise direction as indicated by the black arrows. In order to support the following discussion region of interests in the graphs are indicated with red and orange diamonds.

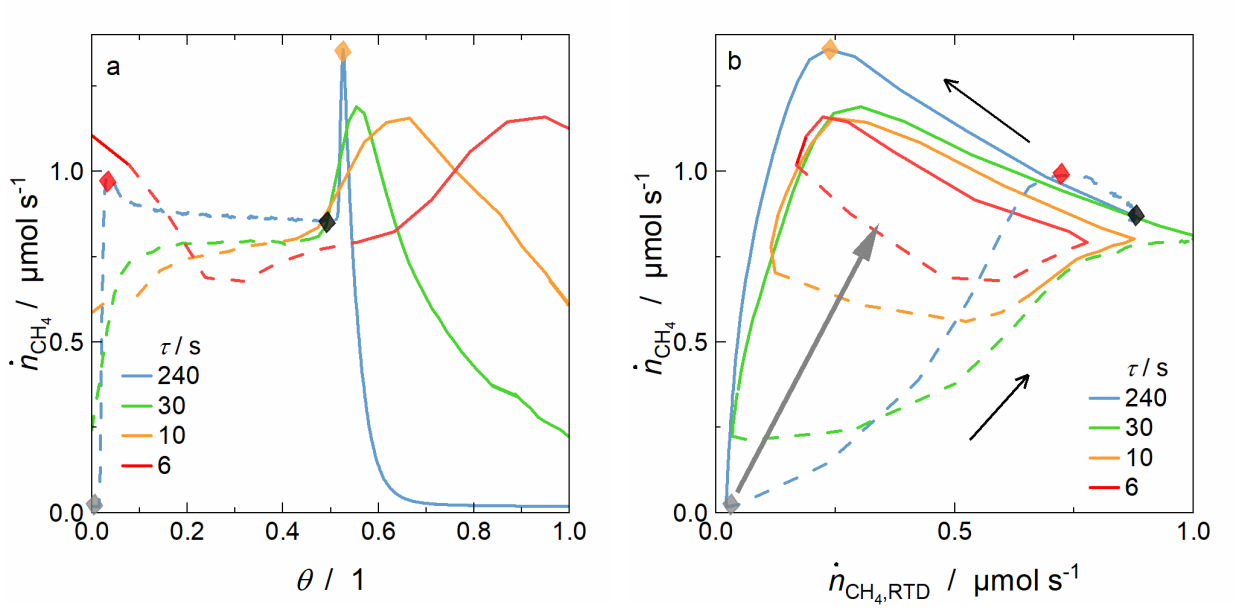

Figure 3: CH_4 outlet molar flow rate for different cycle period durations τ as function of the normalized time within the limit cycle (a) and depicted in the corresponding state space plot (b) (reaction conditions: z = 0.5, 556 K, 2 bar).

It can be seen that the hysteresis is most pronounced for a cycle period duration of 240 s, since the steady-state values are reached for both the CO_x-lean and CO_x-rich phase. This means that no CH_4 is produced during the CO_x-lean phase for over 50 s. For shorter cycle period durations the steady-states are not reached, neither for the measured nor for the expected response, and thus the hysteresis is compressed. As discussed above already, the magnitude decreases for all components with shorter cycle periods, which directly relates to narrowing of the hysteresis. The comparison of the 240 with the 6 s cycle period reveals that the hysteresis is absent for low $\dot{n}_{CH_4,RTD}$ (grey arrow) at short cycle periods, since CH_4 is also formed in the CO_x-lean phase.

From Figure 3b it is apparent that the hysteresis branch-in the CO_x-rich half-period exhibits only a local maximum (red diamond) for a cycle period duration of 240 s. This maximum corresponds to an overshoot in CH_4 formation rate, which is most likely caused by high H_2 coverage prior

switching to the CO_x-rich phase as reported previously.[39] Reduction of the cycle period duration leads to shorter CO_x-lean phases and therefore only partial conversion and subsequent desorption of the reaction intermediates adsorbed at the catalyst surface. Consequently, a certain amount of those intermediates is still adsorbed after switching to the CO_x-rich phase occupying sorption sites and thereby reducing the number of active sites available for H_2 to adsorb. Additionally, CO can only desorb partially from the surface during shorter cycle periods, due to kinetic limitations of the desorption. These effects lower the initial H_2 coverage prior to the CO_x-rich phase and hence, the CH_4 formation rate is reduced leading to a diminishing overshoot in that half-period. At the same time the upper branch, corresponding to the CO_x-lean half-period, remains rather unaffected (orange diamond). Therefore, the CH_4 methanation rate exceeds the value of the steady-state almost during the whole CO_x-lean half-period for short durations, while it approaches zero for long durations. This means that CH_4 formation is favored during the CO_x-lean phase.

This behavior can be explained by formation of two carbon containing intermediates on the catalyst surface, which differ in their reactivity. In particular, upon switching to CO_x-free mixtures a highly reactive species is completely converted with a certain rate independent on the cycle period duration, as indicated by the rather unaffected upper branch and the global maximum of the hysteresis. Consequently, the generation and conversion of the highly reactive species has to be faster than the shortest cycle periods, as enough CH_4 is provided to maintain the global maximum in the response. The existence of a highly reactive species is supported by the observations of different authors.[41–43] Fujita et al.[41] investigated the transient CH_4 response by DRIFTS measurements for CO and CO_2 hydrogenation. They conclude that the maximum resp. overshoot is caused by the hydrogenation of a highly reactive, carbonaceous species adsorbed at the solid surface, which is suggested to contain only carbon (C_α). As the CO containing feed is switched

off, the linearly adsorbed CO molecules desorb releasing sites available for H_2 adsorption during the CO_x-lean half period. This causes a rapid hydrogenation of C_α into CH_4 and therefore the observed overshoot.

The hydrogenation of the less reactive species, in contrast, is strongly affected by the cycle period duration. For $\tau = 240$ s this species can be completely converted to CH_4 and, hence, the respective outlet molar flow rate approaches zero at the end of each half-period. For shorter cycle periods, however, the CO_x-rich phase starts accompanied by adsorption of CO before full conversion of the less reactive surface species into is CH_4 reached. Thus, CH_4 is detected in the outlet stream during the whole limit cycle. The existence of such species is in accordance with the observations of different authors.[41–43]

3.3. Effect of temperature and CO/CO_2 ratio

The response of CH_4 is depicted in Figure 4 for different cycle period durations, temperatures and CO_x feed compositions. Note, that the data of subfigures f and g correspond to those of Figure 1 and Figure 3, respectively.

From Figure 4 it is apparent that the hysteresis branch during CO_x-rich feed composition (lower branch) exhibits a local maximum only for $z = 1$ and 0.5 and a cycle period duration of 240 s (first two columns in Figure 4) before approaching the steady-state. The maximum diminishes for shorter cycle periods and lower z values. Furthermore, a global maximum in CH_4 formation rate occurs under CO_x-lean feed gas composition. For decreasing z values the maximum value decreases, as well, and diminishes completely for small $z = 0$ (pure CO_2 methanation). Therefore, the observed hysteresis for methanation of pure CO ($z = 1$) and CO_2 ($z = 0$) deviate significantly with respect to the occurring maximum and two different reaction mechanisms are likely to occur depending on the CO/CO_2 ratio. For CO methanation we have shown recently that the dynamic

CH_4 response is governed by the presence of a highly reactive carbide species (C_α) assuming the carbide pathway mechanism.[44] In particular, the C_α species are formed at the active surface during the build-up phase under CO methanation conditions (high z values). After switching to the back-transient phase, the C_α compounds are hydrogenated very fast to CH_4, which causes the overshoot in the CH_4 response due to the surplus availability of H_2. Since, C_α species are only formed under CO methanation conditions (high z values), but not significantly for small z values,[41,43] the overshoot is not observed under CO_2 methanation conditions. Specifically, in case of CO_2 methanation Fujita et al.[41] report hydrogenation of less reactive species after switching to pure H_2, which is not accelerated sufficiently to cause an overshoot. Therefore, the CH_4 formation rate decreases monotonously with the CO_2 fraction in the gas phase. For $0 < z < 1$ the amount of C_α scales with z, which affects the extent of the observed overshoot.[39] Consequently, based on the form of the hysteresis the participation of CO and CO_2 during CO_x methanation can be differentiated.

This hypothesis is supported by the observed temperature dependency and the expected impact of temperature on the sorption equilibrium and the surface reaction rates. At higher temperatures the amount of adsorbed carbonaceous species is reduced and, thus, more active sites are available for H_2.[43,45] Since the reaction rate increases as well, as becomes apparent from the scale of the ordinate axis, both factors lead to an enhanced hydrogenation rate of adsorbed carbonaceous species at the catalyst surface during the CO_x-lean phase. Therefore, smaller coverage degrees regarding those species remain at the end of the CO_x-lean half-period, which correspond to lower CH_4 formation rates. Hence, the hysteresis expands with increasing temperatures towards smaller CH_4 outlet molar flow rates.

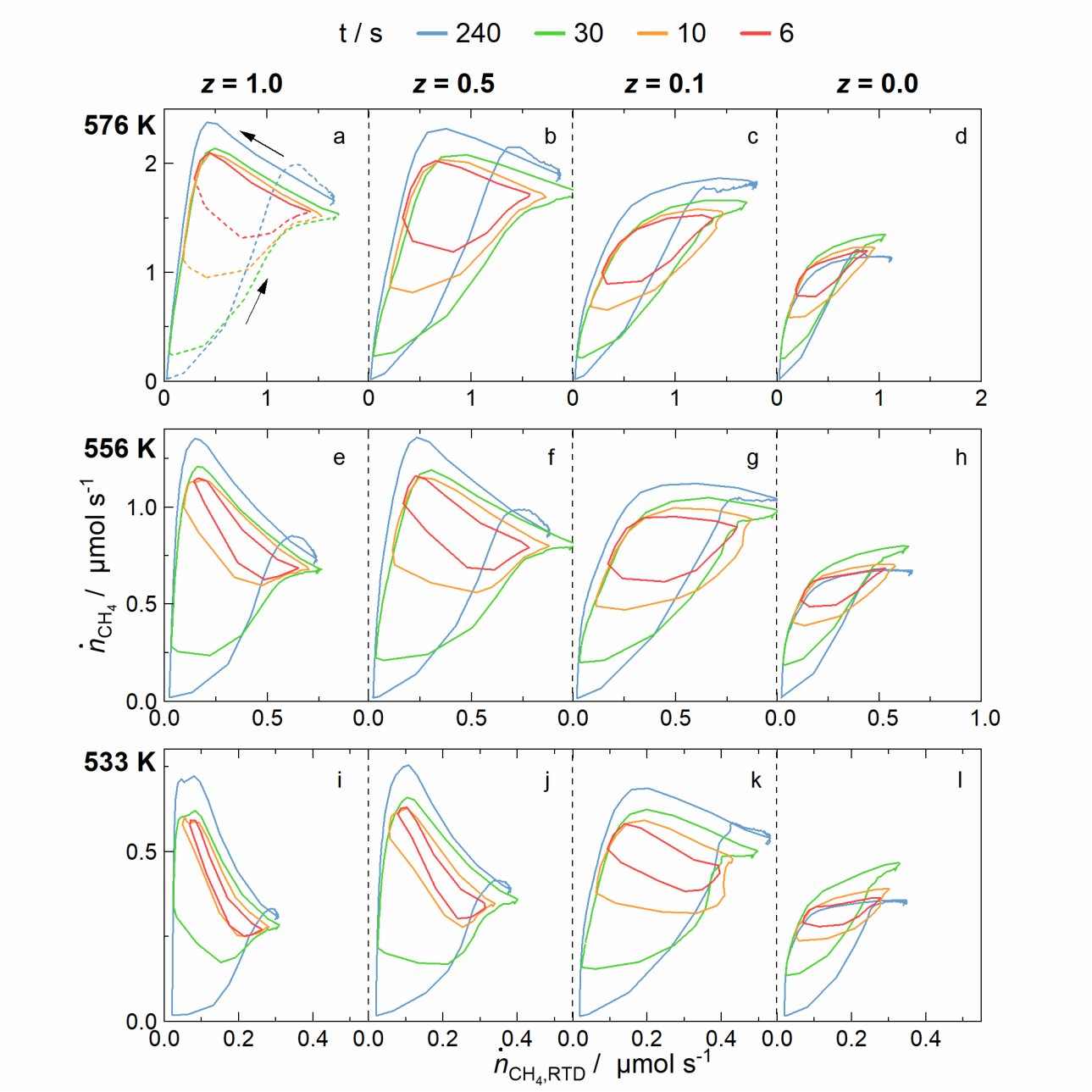

Figure 4: CH_4 outlet molar flow rates for different cycle period durations τ, temperatures T and CO_x feed compositions z (reaction pressure: 2 bar).

In conclusion, the carbide pathway mechanism is evident due to the presence of C_α species for CO methanation, while the H_2 assisted pathway mechanism is likely for CO_2 methanation, since

C_α species are not observed. These mechanistic findings are in agreement with literature on CO/CO_2 hydrogenation on Ni catalyst.[2,46,47]

3.4. Performance enhancement

From the frequency response results one may hypothesize that it is possible to increase the average CH_4 formation rate by decreasing the cycle period duration, especially at low temperatures and CO containing feed gas mixtures. Therefore, Figure 5 displays the reactor performance in terms of the rate enhancement factor E. Obviously, for $\tau = 240$ s the lowest reactor performance is achieved, while it increases for shorter durations. The extent of improvement, though, depends on the CO/CO_2 ratio fed, increasing from pure CO_2 to pure CO methanation.

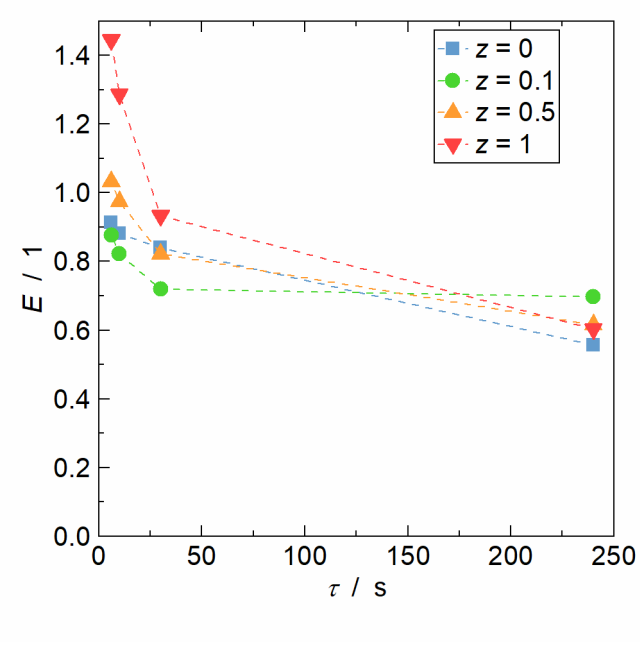

Figure 5: Rate enhancement factor E as function of the cycle period duration τ and CO/CO_2 feed gas ratio z at a temperature of 556 K.

In comparison, Table 3 summarizes the rate enhancement factor E for the hydrogenation of CO or CO_2 from various literature reports. For the CO methanation the CH_4 yield is reported to

increase by reducing the cycle period duration, regardless of the catalytic system.[31–33] Hence, it is likely that the observed rate enhancement is caused by the selective activation of the highly reactive C_α intermediate species during the CO_x lean phase. For example, Yadav and Rinker[31] observed a rate enhancement only for cycle periods shorter than 16 s with a comparable catalyst, which suggests that they also primarily activate the highly reactive C_α species, while the less reactive species remain in a dynamic equilibrium on the catalyst surface. For CO_2 methanation, in contrast, the reaction rate can also be increased by shorter cycle periods, but hardly exceeds the corresponding steady-state values,[34,35] what we observe as well (Figure 5).

Table 3: Rate enhancement reported in literature in comparison to the present work for hydrogenation of CO or CO_2.

Gas mixtures		Reaction system	Catalyst	τ	s	E	Reference
I	II			s	1	1	
CO	H_2	CO methanation	Ni/Al_2O_3	12 - 24	0.25 - 0.45	0.58 - 1.06	Yadav and Rinker[31]
H_2/CO	H_2		Ni/SiO_2	6 - 100	0.5	1.33 - 1.66	Klusácek and Stuchlý[32]
$H_2/CO/Ar$	H_2		Ni/Al_2O_3	6 - 240	0.5	0.6 - 1.44	this work
$H_2/CO_2/He$	H_2/He	CO_2 methanation	Ru/TiO_2	300 - 5700	0.5	0.79 - 1.02	Marwood et al.[34]
CO_2/Ar	H_2/He		Ni/Al_2O_3	10 - 120	0.2 - 0.8	0.08 - 0.87	Kreitz et al.[35]
$H_2/CO_2/Ar$	H_2		Ni/Al_2O_3	6 - 240	0.5	0.56 - 0.91	this work
$H_2/CO/He$	H_2/He	Fischer-Tropsch	Co/SiO_2	60 - 600	0.5, 0.8	0.75 - 7	Adesina et al.[33]

The rate enhancement potential is discussed for periodic changes in the inlet gas composition, which is most studied in literature (see Table 3), as well. However, from the results reported in

Figure 4 a strong impact of temperature on the periodic response becomes evident. Hence, periodic changes in temperature most probably allow further enhancement in performance.

4 CONCLUSION

The influence of the cycle period duration of the inlet gas composition on the unsteady-state CO_x methanation reaction was investigated under realistic conditions. The dynamic experiments were conducted by periodically exchanging a gas mixture containing H_2 and a certain CO/CO_2 ratio with a CO_x-free gas feed keeping the H_2 concentration constant. Different CO/CO_2 ratios were studied between pure CO and pure CO_2 in order to investigate the competing effects of both carbon oxides and deduce experimental insights for flexible operation. The frequency response of the components was evaluated in the quasi-steady-state (qss), full-transient state (fts) and relaxed steady-state (rss) regime, putting emphasis on CH_4. The following conclusions can be deduced from the obtained results:

- Based on the applied cycle period durations each component exhibits a characteristic dynamic behavior. For longer cycle periods the components remain in the *qss* regime approaching the respective steady-state values in each half-period. Reducing the cycle period duration leads to a shift towards the *fts* are even the *rss* regime, which becomes most pronounced for H_2O and the shortest investigated cycle period.
- An analysis of the magnitude reveals that the frequency response of the reactants differ from that of the products. While the reactants follow the internal standard and thus the RTD, the products exhibit a decline of the magnitude with decreasing cycle period durations with a larger slope. This low-pass behavior agrees with predictions for more simple cases. Furthermore, storage of the formed products in the system by adsorption at the catalyst surface is also observed in the frequency response by an even more

pronounced damping of the input fluctuations, expressed by a steeper drop of the magnitude.

- The form of the hysteresis in the state-space plot is significantly correlated with the presence of CO, the temperature and the cycle period duration. The interpretation of the state space plots supports the presence of reactive C_α species at the catalyst surface. These species cause CH_4 formation rates exceeding values expected from steady-state experiments and appear to require CO in the gas phase.
- The highly reactive C_α species can selectively be hydrogenated into CH_4 by a reduction of the cycle period duration, since the less reactive surface species become rather inert. This is likely to be the reason for the enhancement of the average CH_4 formation rate under concentration forcing conditions with respect to the steady-state, which is reported for methanation of CO, but not for CO_2.[31,32] The results obtained in this work for simultaneous methanation of CO and CO_2 underline the importance of CO for the enhancement in average methanation rate and therefore the hypothesis of reactive C_α species, as well.

Our results are based on measuring the transient reactor response in form of the outlet gas composition. The application of evaluation procedures based on material balances allows us to deduce molar flow rates for the relevant components present in the gas phase. Therefore, the conclusions drawn regarding kinetic processes taking place or species present at the surface are not directly verified by measurements. For this purpose, complementary *in situ* and *operando* experiments are required for the unsteady-state CO_x methanation, in order to verify the discussed hypotheses in future work. In particular, X-ray absorption spectroscopy combined with modulation excitation spectroscopy (XAS-MES), recently reported by Serrer et al.,[48] appears to be promising

to link the periodic response of the gas phase measured via the periodic transient kinetics (PTK) method with the dynamics of kinetic processes at the solid surfaces. Those combined experiments provide the basis for the full kinetic understanding of the dynamic catalyst behavior including the storage capacity of the reactants at the active and support material and, hence, for development and validation of a micro kinetic model applicable to the unsteady-state methanation reaction.

AUTHOR INFORMATION

Corresponding Author

Robert Güttel

Tel.: 49 731/50-25700

E-mail address: robert.guettel@uni-ulm.de

Author Contributions

The manuscript was written through contributions of all authors in the following manner: **Dominik Meyer**: Conceptualization, Conducting experiments, Data evaluation, Writing original draft, Writing review and editing; **Jannik Schumacher**: Scientific discussion, Writing review and editing; **Jens Friedland**: Scientific discussion, Writing review and editing; **Robert Güttel**: Scientific discussion, Conceptualization, Project administration, Supervision, Writing original draft, Writing review and editing. All authors have given approval to the final version of the manuscript.

ACKNOWLEDGMENT

The authors want to thank Sasol Germany GmbH for providing the support material.

ABBREVATIONS

CO_x, CO/CO_2; fts, full-transient state; MS, mass spectrometer; PtG, Power-to-Gas; PTK, Periodic Transient Kinetics; qss, quasi-steady-state; SNG, Synthetic or Substitute Natural Gas; rss, relaxed steady-state; RTD, residence time distribution

REFERENCES

(1) Kalz, K. F.; Kraehnert, R.; Dvoyashkin, M.; Dittmeyer, R.; Gläser, R.; Krewer, U.; Reuter, K.; Grunwaldt, J.-D. Future challenges in heterogeneous catalysis:Understanding catalysts under dynamic reaction conditions. *ChemCatChem* **2017**, *9* (1), 17–29. DOI: 10.1002/cctc.201600996.

(2) Vogt, C.; Monai, M.; Kramer, G. J.; Weckhuysen, B. M. The renaissance of the Sabatier reaction and its applications on earth and in space. *Nat. Catal.* **2019**, *2* (3), 188–197. DOI: 10.1038/s41929-019-0244-4.

(3) Götz, M.; Lefebvre, J.; Mörs, F.; McDaniel Koch, A.; Graf, F.; Bajohr, S.; Reimert, R.; Kolb, T. Renewable Power-to-Gas:A technological and economic review. *Renew. Energy* **2016**, *85*, 1371–1390. DOI: 10.1016/j.renene.2015.07.066.

(4) Schöß, M. A.; Redenius, A.; Turek, T.; Güttel, R. Chemische Speicherung regenerativer elektrischer Energie durch Methanisierung von Prozessgasen aus der Stahlindustrie. *Chem. Ing. Tech.* **2014**, *86* (5), 734–739. DOI: 10.1002/cite.201300086.

(5) Meyer, D.; Schumacher, J.; Friedland, J.; Güttel, R. Hydrogenation of CO/CO_2 mixtures on nickel catalysts: Kinetics and flexibility for nickel catalysts. *Ind. Eng. Chem. Res.* **2020**, *59* (33), 14668–14678. DOI: 10.1021/acs.iecr.0c02072.

(6) Meyer, D.; Friedland, J.; Schumacher, J.; Güttel, R. The periodic transient kinetics method for investigation of kinetic process dynamics under realistic conditions: Methanation as an example. *Chem. Eng. Res. Des.* **2021**, *173*, 253–266. DOI: 10.1016/j.cherd.2021.07.011.

(7) Meyer, D.; Friedland, J.; Kohn, T.; Güttel, R. Transfer functions for periodic reactor operation:Fundamental methodology for simple reaction networks. *Chem. Eng. Technol.* **2017**, *40* (11), 2096–2103. DOI: 10.1002/ceat.201700122.

(8) Yakhnin, V. Z.; Menzinger, M. Moving hot spots and resonance in adiabatic packed-bed reactors. *AlChE J.* **1998**, *44* (5), 1222–1225. DOI: 10.1002/aic.690440521.

(9) van Doesburg, H.; Jong, W. A. de. Transient behaviour of an adiabatic fixed-bed methanator—II. *Chem. Eng. Sci.* **1976**, *31* (1), 53–58. DOI: 10.1016/0009-2509(76)85008-7.

(10) van Doesburg, H.; Jong, W. A. de. Transient behaviour of an adiabatic fixed-bed methanator—I. *Chem. Eng. Sci.* **1976**, *31* (1), 45–51. DOI: 10.1016/0009-2509(76)85007-5.

(11) Kulkarni, M. S.; Dudukovic', M. P. Dynamics of gas phase and solid phase reactions in fixed bed reactors. *Chem. Eng. Sci.* **1996**, *51* (11), 3083–3088. DOI: 10.1016/0009-2509(96)00201-1.

(12) Bremer, J.; Sundmacher, K. Operation range extension via hot-spot control for catalytic CO_2 methanation reactors. *React. Chem. Eng.* **2019**, *4* (6), 1019–1037. DOI: 10.1039/C9RE00147F.

(13) Theurich, S.; Rönsch, S.; Güttel, R. Transient Flow Rate Ramps for Methanation of Carbon Dioxide in an Adiabatic Fixed-Bed Recycle Reactor. *Energy Technol.* **2020**, *8* (3), 1901116. DOI: 10.1002/ente.201901116.

(14) Matthischke, S.; Rönsch, S.; Güttel, R. Start-up Time and Load Range for the Methanation of Carbon Dioxide in a Fixed-Bed Recycle Reactor. *Ind. Eng. Chem. Res.* **2018**, *57* (18), 6391–6400. DOI: 10.1021/acs.iecr.8b00755.
(15) Matthischke, S.; Krüger, R.; Rönsch, S.; Güttel, R. Unsteady-state methanation of carbon dioxide in a fixed-bed recycle reactor — Experimental results for transient flow rate ramps. *Fuel Process. Technol.* **2016**, *153*, 87–93. DOI: 10.1016/j.fuproc.2016.07.021.
(16) Try, R.; Bengaouer, A.; Baurens, P.; Jallut, C. Dynamic modeling and simulations of the behavior of a fixed-bed reactor-exchanger used for CO_2 methanation. *AlChE J.* **2017**, *38* (5), 2039. DOI: 10.1002/aic.15874.
(17) Mutz, B.; Gänzler, A. M.; Nachtegaal, M.; Müller, O.; Frahm, R.; Kleist, W.; Grunwaldt, J.-D. Surface oxidation of supported Ni particles and its impact on the catalytic performance during dynamically operated methanation of CO_2. *Catalysts* **2017**, *7* (9), 279. DOI: 10.3390/catal7090279.
(18) Soong, Y.; Krishna, K.; Biloen, P. Catalyst aging studied with isotopic transients: Methanation over Raney Nickel. *J. Catal.* **1986**, *97* (2), 330–343.
(19) Zimmermann, R. T.; Bremer, J.; Sundmacher, K. Optimal catalyst particle design for flexible fixed-bed CO_2 methanation reactors. *Chem. Eng. J.* **2020**, *387*, 123704. DOI: 10.1016/j.cej.2019.123704.
(20) Hudgins, R. R.; Silveston, P. L.; Renken, A.; Matros, Y. S. Introduction. In *Periodic operation of reactors,* 1st ed.; Silveston, P. L., Hudgins, R. R., Eds.; Elsevier, 2013; pp 1–22. DOI: 10.1016/B978-0-12-391854-3.00001-2.
(21) Bailey, J. E. Periodic operation of chemical reactors:A Review. *Chem. Eng. Commun.* **1974**, *1* (3), 111–124. DOI: 10.1080/00986447408960421.
(22) Silveston, P. L.; Hudgins, R. R., Eds. *Periodic operation of reactors*, 1st ed.; Elsevier, 2013.
(23) Renken, A. The use of periodic operation to improve the performance of continuous stirred tank reactors. *Chem. Eng. Sci.* **1972**, *27* (11), 1925–1932. DOI: 10.1016/0009-2509(72)87051-9.
(24) Schädlich, K.; Hoffmann, U.; Hofmann, H. Periodical operation of chemical processes and evaluation of conversion improvements. *Chem. Eng. Sci.* **1983**, *38* (9), 1375–1384. DOI: 10.1016/0009-2509(83)80073-6.
(25) Matros, Y. S. Unsteady performance of heterogeneous catalytic reactions. *React Kinet Catal Lett* **1987**, *35* (1-2), 425–435. DOI: 10.1007/BF02062177.
(26) van Neer, F. J.; Kodde, A. J.; Den Uil, H.; Bliek, A. Understanding of resonance phenomena on a catalyst under forced concentration and temperature oscillations. *Can. J. Chem. Eng.* **1996**, *74* (5), 664–673.
(27) Petkovska, M.; Nikolić, D.; Marković, A.; Seidel-Morgenstern, A. Fast evaluation of periodic operation of a heterogeneous reactor based on nonlinear frequency response analysis. *Chem. Eng. Sci.* **2010**, *65* (11), 3632–3637. DOI: 10.1016/j.ces.2010.03.011.
(28) Petkovska, M.; Seidel-Morgenstern, A. Evaluation of periodic processes. In *Periodic operation of reactors,* 1st ed.; Silveston, P. L., Hudgins, R. R., Eds.; Elsevier, 2013; pp 387–413. DOI: 10.1016/B978-0-12-391854-3.00014-0.
(29) Currie, R.; Nikolić, D.; Petkovska, M.; Simakov, D. S. CO_2 conversion enhancement in a periodically operated sabatier reactor:Nonlinear Frequency Response Analysis and Simulation-based Study. *Isr. J. Chem.* **2018**, *58* (6-7), 762–775. DOI: 10.1002/ijch.201700134.
(30) Nikačević, N.; Todić, B.; Mandić, M.; Petkovska, M.; Bukur, D. B. Optimization of forced periodic operations in milli-scale fixed bed reactor for Fischer-Tropsch synthesis. *Catal. Today* **2020**, *343*, 156–164. DOI: 10.1016/j.cattod.2018.12.032.
(31) Yadav, R.; Rinker, R. G. The efficacy of concentration forcing. *Chem. Eng. Sci.* **1989**, *44* (10), 2191–2195. DOI: 10.1016/0009-2509(89)85153-X.

(32) Klusáček, K.; Stuchlý, V. Increasing of carbon monoxide methanation rate by forced feed composition cycling. *Catal. Today* **1995**, *25* (2), 169–174. DOI: 10.1016/0920-5861(95)00106-P.
(33) Adesina, A. A.; Hudgins, R. R.; Silveston, P. L. Influence of concentration waves on the fischer-tropsch reaction. *J. Chem. Technol. Biotechnol.* **1991**, *50* (4), 535–547. DOI: 10.1002/jctb.280500410.
(34) Marwood, M.; van Vyve, F.; Doepper, R.; Renken, A. Periodic operation applied to the kinetic study of CO_2 methanation. *Catal. Today* **1994**, *20* (3), 437–448. DOI: 10.1016/0920-5861(94)80137-1.
(35) Kreitz, B.; Friedland, J.; Güttel, R.; Wehinger, G. D.; Turek, T. Dynamic methanation of CO_2 – effect of concentration forcing. *Chem. Ing. Tech.* **2019**, *91* (5), 576–582. DOI: 10.1002/cite.201800191.
(36) Klose, J.; Baerns, M. Kinetics of the methanation of carbon monoxide on an alumina-supported nickel catalyst. *J. Catal.* **1984**, *85* (1), 105–116. DOI: 10.1016/0021-9517(84)90114-3.
(37) Gao, J.; Wang, Y.; Ping, Y.; Hu, D.; Xu, G.; Gu, F.; Su, F. A thermodynamic analysis of methanation reactions of carbon oxides for the production of synthetic natural gas. *RSC Adv.* **2012**, *2* (6), 2358–2368. DOI: 10.1039/c2ra00632d.
(38) Shekhtman, S. O.; Yablonsky, G. S. Thin-Zone TAP reactor versus differential PFR: Analysis of concentration nonuniformity for gas−solid systems. *Ind. Eng. Chem. Res.* **2005**, *44* (16), 6518–6522. DOI: 10.1021/ie050554g.
(39) Meyer, D.; Friedland, J.; Schumacher, J.; Güttel, R. Hydrogenation of CO/CO_2 mixtures under unsteady-state conditions: Effect of the carbon oxides on the dynamic methanation process. In Press. *Chem. Eng. Sci.* **2021**, 117405. DOI: 10.1016/j.ces.2021.117405.
(40) Zarfl, J.; Ferri, D.; Schildhauer, T. J.; Wambach, J.; Wokaun, A. DRIFTS study of a commercial Ni/γ-Al_2O_3 CO methanation catalyst. *Appl. Catal., A* **2015**, *495*, 104–114. DOI: 10.1016/j.apcata.2015.02.005.
(41) Fujita, S.-I.; Nakamura, M.; Doi, T.; Takezawa, N. Mechanisms of methanation of carbon dioxide and carbon monoxide over nickel/alumina catalysts. *Appl. Catal., A* **1993**, *104* (1), 87–100. DOI: 10.1016/0926-860X(93)80212-9.
(42) Efstathiou, A. M.; Bennett, C. O. Surface species on Rh/Al_2O_3 during CO/H_2 reaction studied by transient techniques. *Chem. Eng. Commun.* **1989**, *83* (1), 129–146. DOI: 10.1080/00986448908940658.
(43) Underwood, R. P.; Bennett, C. O. The COH_2 reaction over nickel-alumina studied by the transient method. *J. Catal.* **1984**, *86* (2), 245–253. DOI: 10.1016/0021-9517(84)90370-1.
(44) Meyer, D.; Friedland, J.; Schumacher, J.; Gäßler, M. G.; Güttel, R. Hydrogenation of CO/CO2 mixtures under unsteady-state conditions: Effect of the carbon oxides on the dynamic methanation process. *Chem. Eng. Sci.* **2021**, 117405. DOI: 10.1016/j.ces.2021.117405.
(45) Falbo, L.; Visconti, C. G.; Lietti, L.; Szanyi, J. The effect of CO on CO_2 methanation over Ru/Al_2O_3 catalysts:A combined steady-state reactivity and transient DRIFT spectroscopy study. *Appl. Catal., B* **2019**, *256*, 117–791. DOI: 10.1016/j.apcatb.2019.117791.
(46) Gao, J.; Liu, Q.; Gu, F.; Liu, B.; Zhong, Z.; Su, F. Recent advances in methanation catalysts for the production of synthetic natural gas. *RSC Adv* **2015**, *5* (29), 22759–22776. DOI: 10.1039/C4RA16114A.
(47) Miao, B.; Ma, S. S. K.; Wang, X.; Su, H.; Chan, S. H. Catalysis mechanisms of CO_2 and CO methanation. *Catal. Sci. Technol.* **2016**, *6* (12), 4048–4058. DOI: 10.1039/C6CY00478D.
(48) Serrer, M.-A.; Gaur, A.; Jelic, J.; Weber, S.; Fritsch, C.; Clark, A. H.; Saraçi, E.; Studt, F.; Grunwaldt, J.-D. Structural dynamics in Ni–Fe catalysts during CO_2 methanation – role of iron oxide clusters. *Catal. Sci. Technol.* **2020**, *10* (22), 7542–7554. DOI: 10.1039/D0CY01396J.